

Description of PtAu Potential

C. J. O'Brien, C. M. Barr, P. M. Price, K. Hattar, and S. M. Foiles,
Journal of Materials Science 53(4) 2017, 2911–2927.

DOI [10.1007/s10853-017-1706-1](https://doi.org/10.1007/s10853-017-1706-1)

Corresponding author: cjobrie@sandia.gov

April 14, 2018

Abstract

New Embedded Atom Method (EAM) interatomic potentials are developed for Pt, Au, and the PtAu binary alloy. The potential is available in the setfl format. In LAMMPS, this is an EAM/Alloy-style potential.

1 Pt-Au Potential Development

1.1 Calculation of Reference Structures

Due to the lack of measured properties for the PtAu alloy, we instead rely on Density Functional Theory to provide forces and energies for ordered and disordered configurations with which the potentials will be parameterized; This strategy is referred to as force matching [1]. In force matching, two databases are generated, one for parameterization and one for validation. The databases consist of a wide variety of configurations that represent a range of conditions at which the potential might be applied. Using the force-matching approach, individual properties are not reproduced, but rather the goal is to fit the interatomic forces and energies of a wide variety of systems. Since the fit must be applicable to grain boundaries that contain disordered regions at the boundary, it is necessary to fit the potentials for disordered solids in addition to crystalline phases. The actual structures do not need to be equilibrium ones, or even thermodynamically stable states as the DFT calculations only provide energies and forces with which to fit the potential.

Single element potentials are fit to a small range of lattice constants about equilibrium for the FCC, BCC, HCP, diamond, and disordered FCC structures. The disordered FCC structures included random displacements up to 0.1 Å. Also included in the database are multiple sample configurations of a liquid state at 2000 K. The fitting database for the alloy potential consists of a variety of structures including configurations of the liquid PtAu alloy at 2000 K, an FCC PtAu alloy with random displacements of up to 0.1 Å, a range of lattice constants for the ordered compounds L_{12} , B_1 , and L_{20} .

1.2 Functional form of the Potential

The cutoff function Ξ is applied to both the density and pair potential and takes the form

$$\Xi(\chi) = -6\chi^5 + 15\chi^4 - 10\chi^3 + 1 \quad \text{where} \quad \chi(r, r_c) = \frac{r - r_c}{r_{\text{cut}} - r_c} H(r_c). \quad (1)$$

The function H is the Heaviside step function switching at the inner cutoff r_c , and the global cutoff for the potential is r_{cut} . The pair and density functions each have their own inner cutoff radius defined as r_p and r_d , respectively.

The functional form of the pair potential employed is that of Morse [2],

$$\phi(r) = D_e \left\{ \left[1 - e^{-a_m(r-r_0)} \right]^2 - 1 \right\} \cdot \Xi(r, r_p), \quad (2)$$

where D_e and a_m are fitting parameters, and r_0 is the equilibrium bond distance as determined from DFT calculations. The electron density function is a simple exponential,

$$\rho(r) = \rho_0 e^{-\frac{r-r_0}{\lambda_0}} \cdot \Xi(r, r_d), \quad (3)$$

where ρ_0 and λ_0 are fitting parameters.

The embedding function is derived as done by Foiles [3] starting with the expression for the total energy of the EAM potential

$$E_{\text{tot}} = \sum_i F_i(\rho_i) + \frac{1}{2} \sum_{i,j} \phi_{ij}(r_{ij}) \quad \text{where} \quad \rho_i = \sum_{j \neq i} \rho(r_{ij}). \quad (4)$$

Foiles replaced the total energy function E_{tot} with the function from the Rose equation of state for metals [4] and solved Eq. 4 for the embedding functional. The Rose equation of state takes the form

$$E_{\text{Rose}}(r) = E_0 (1 + a^*) e^{-a^*}, \quad (5)$$

where E_0 is the cohesive energy and

$$a^* \equiv \frac{a - a_0}{a_0 \lambda_R}. \quad (6)$$

The a_0 term is the DFT calculated lattice constant and $\lambda_R = \sqrt{E_0 / (9\Omega B)}$. This term contains the cohesive energy (E_0), bulk modulus (B), and atomic volume (Ω), which are obtained from experiments or, in this case, first-principles calculations. With the Rose equation of state incorporated into the potential, the λ_R term is guaranteed to be reproduced by the fit.

1.3 Procedure for Fitting the Potential

The actual fitting of the nine parameters was carried out using the Dakota [5] software package developed at Sandia National Laboratories. The optimization utilized the gradient and hessian free Collony pattern search algorithm. After each optimization step, Dakota called LAMMPS [6] that was used to determine the error between the energies and forces

calculated with the EAM potential to the reference data. DAKOTA optimized the parameters until the change in the error (root of the sum of squares of the differences) was less than 1×10^{-3} .

The Rose equation of state is used to constrain the energy versus lattice constant relationship, the λ_R term is fixed using the DFT calculated values for each element. Consequently, there is some deviation in the parameters for binding energy E_0 , lattice constant a_0 , and bulk modulus B , due to the λ_R quantity being constrained, rather than the constituent properties being restricted individually.

The maximum electron density is 50 \AA^{-3} , and the cutoff for the potentials are 5.50 \AA for Pt, and 5.75 \AA for Au and PtAu. Since the cutoff parameter must be fixed initially in this scheme, a range of values were used and fits were attempted for each.

1.4 Results and Validation of Fits

Plots of the pair potentials, electron densities, and embedding functionals obtained by the fitting procedure are provided in Figs. 2–3. Validation of the elemental potentials is carried out for a number of cases, many are found in Table 1, in addition to comparisons to independent data of the elemental liquid at 2000 K and the FCC structure with random displacements. Specific geometries of interest are also included such as the intrinsic stacking fault, the $\Sigma 3(111)(110)$ (coherent twin) boundary, self-interstitial, vacancy, and the (111), (100), and (110) surfaces.

The force matching approach relies on the accuracy of the first principles calculations used to obtain forces and energies. However, there are inherent weaknesses in the GGA approach that result in deviation from experiment. For instance, GGA is known to calculate smaller cohesive energies than measured, and larger lattice constants. It is well known that the vacancy formation energy is poorly matched by GGA [7]. Consequently, the vacancy configuration was excluded from the fitting database, but is included in the validation database. Interestingly, the value of the vacancy formation energies calculated by the potential, reported in Table 1, are in general agreement with experimental values.

The validation database for the alloy potential includes independent data for the PtAu liquid and random PtAu FCC alloy. The overall error of the alloy fit to the parameterization database for energies and forces are 2.1796×10^{-2} and 5.3216×10^{-1} , respectively; Compare these error values to those obtained from applying the potential to the validation database of 9.2593×10^{-3} and 7.0764×10^{-1} . After validation of the binary fit, a number of tests were conducted to study the range of applicability of the potential for a number of relevant cases designed to represent grain boundary and surface segregation. The results of these tests are reported in Table 2. Although the absolute errors are rather large for segregation, it was deemed to be acceptable as the sign of the segregation energy and the relative magnitudes are similar. The largest errors present in the table occur for the test of site segregation energies to the $\Sigma 5$ grain boundary. The large errors in the smallest segregation energies is to be expected as the small energy change makes it more difficult to obtain an accurate measure of the small change in system energy. The preference for surface segregation of Au on to Pt surfaces predicted by the potential is Reassuringly, the bulk site-substitution energies are in excellent agreement. A further test of the behavior of the potential was made by constructing a phase diagram for the alloy as illustrated in Fig. 4. The solubility values are in very good

agreement with experimental phase diagrams reported in the literature.

1.5 Coefficients of Fits to Analytical Functions

The coefficients of the parameters in Eqs. 1–3 need to generate the elemental potentials are found in Table 3, and the parameters need for the Pt-Au pair potential are found in Table 4.

2 Polynomial Fits to Properties of the PtAu Potential

The chemical potential difference $\Delta\mu$ at 775 K between Pt and Au is expressed in terms of the absolute atomic concentration c of Au in Pt at 775 K is given in units of eV as

$$\Delta\mu(775\text{ K}) = \ln\left(\frac{c}{3.570,602 \times 10^{-19}}\right) / -15.133,08, \quad (7)$$

where $c \leq 0.01$, the solubility limit.

Polynomial fit of the lattice constant $a(T)$ with respect to temperature is reported in Table 5 using the fitting function:

$$f(T) = AT^3 + BT^2 + CT + D. \quad (8)$$

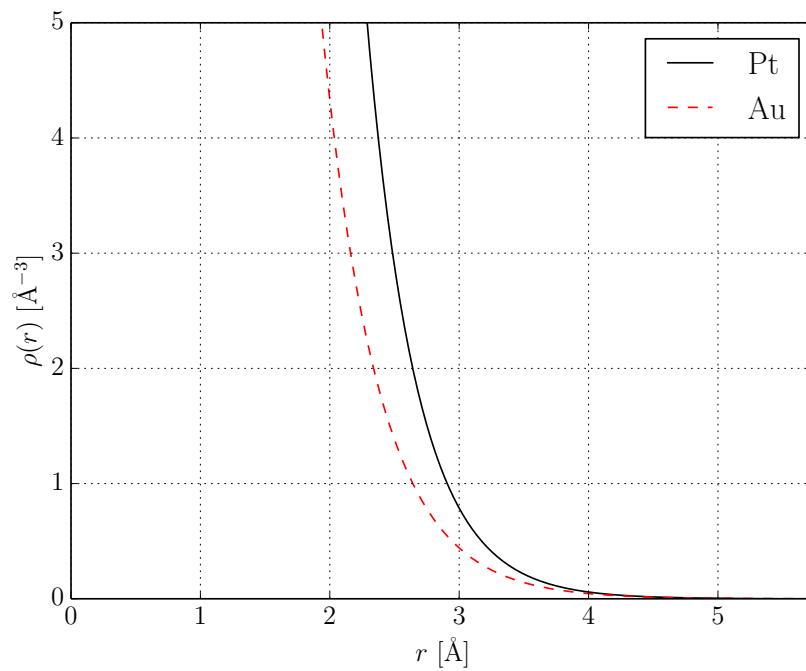


Figure 1: Electron densities for single element potentials.

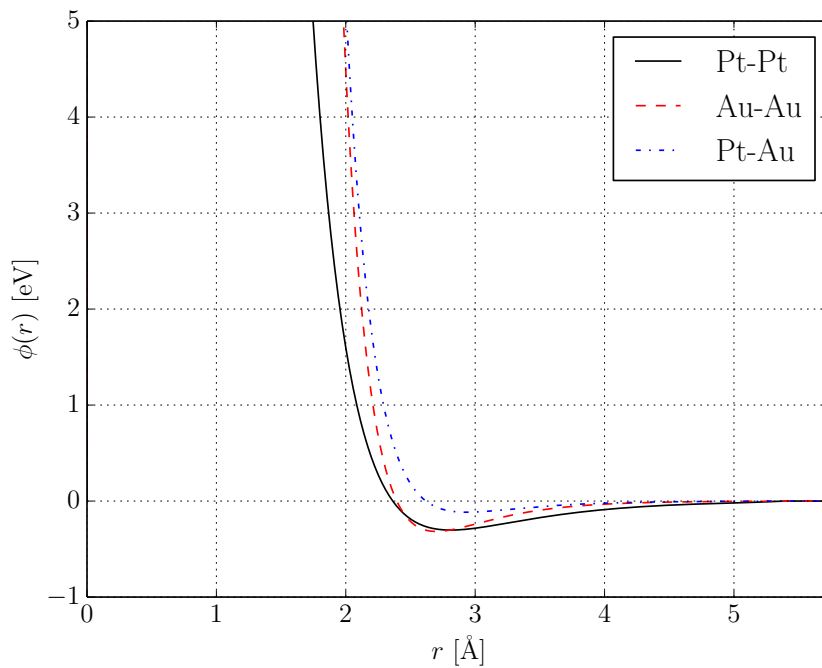


Figure 2: Pair potentials.

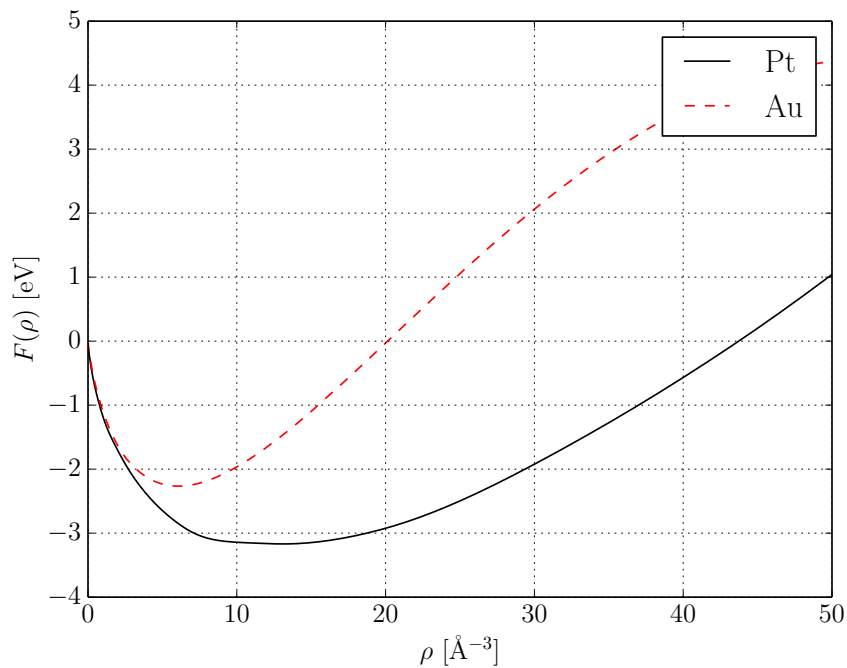


Figure 3: Embedding energies for single element potentials.

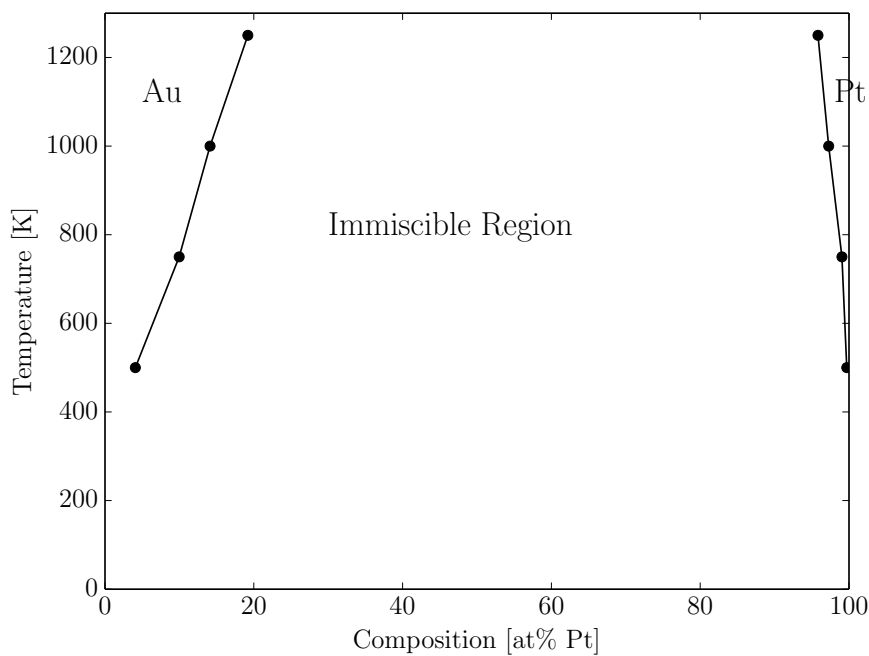


Figure 4: Partial phase diagram of the PtAu system as calculated via the potential developed for this work.

Table 1: Sample values resulting from the fit of single element potentials. The parameters are: E_0 : binding energy; a_0 : lattice constant; B : bulk modulus; ISF: Intrinsic Stacking Fault energy; Twin: $\Sigma 3(111)(1\bar{1}0)$ grain boundary energy; Vac: Relaxed vacancy energy in FCC lattice; Int: Relaxed self interstitial energy in FCC lattice; C_{xx} : Compliance coefficients; B : bulk modulus (calculated with $\frac{1}{3}(C_{11} + 2C_{12})$). Energies are given in eV, surface energies in $\text{mJ} \cdot \text{m}^{-2}$, lattice constants in \AA , and pressures in MPa.

Property	Pt			Au		
	DFT	MD	Ref	DFT	MD	Ref
Fit						
E_0	-5.5057	-5.5050	-5.77 ^b	-3.0374	-3.0374	-3.93 ^b
a_0	3.9764	3.9757	3.92 ^a	4.1537	4.1537	4.08 ^a
B	235.9186	236.0700	283 ^c	146.1305	146.0097	167 ^c
E Error	—	1.8124×10^{-2}	—	—	8.0244×10^{-3}	—
F Error	—	5.7046×10^{-1}	—	—	2.8579×10^{-1}	—
Validation						
$E_{\text{BCC}} - E_{\text{FCC}}$	0.0764	0.0571	—	0.0085	0.0366	—
ISF	307.2131	168.0494	332 ^d	43.6539	67.8987	45 ^d , 50 ^f
Twin	117.6568	33.4571	161 ^d	10.2408	55.2048	23 ^d
Vac	0.6848	1.9773	1.51 ^e	0.4708	1.2225	0.95 ^e
Int	5.3159	4.2845	—	3.0537	3.7485	—
$\gamma(100)$	1833.6088	1742.8123	2480 ^g	954.3534	667.0252	1710 ^g
$\gamma(110)$	1884.3808	1884.3808	—	922.0133	723.9978	1790 ^g
$\gamma(111)$	1464.8728	1649.2121	2350 ^g	707.9624	617.3931	1610 ^g
C_{11}	279.2820	264.3480	347 ^c	146.4985	168.4316	186 ^c
C_{12}	214.2369	221.9309	251 ^c	145.9465	134.7988	157 ^c
C_{44}	65.8006	68.7821	76.5 ^c	25.5122	44.2999	42 ^c
E Error	—	1.8809×10^{-2}	—	—	1.0272×10^{-2}	—
F Error	—	4.1539×10^{-1}	—	—	3.1137×10^{-1}	—

^a Ref. 8

^b Ref. 9

^c Ref. 10

^d Ref. 11

^e Ref. 12

^f Ref. 13 and references therein

^g Ref. 14

Table 2: Testing of PtAu potential in situations relevant to the current study. The $\Sigma 5$ substitution test compares the energy differences for DFT and MD calculations for the energy difference (in eV) between a reference site away from the $\Sigma 5(310)$ tilt grain boundary and an atom in one of four non-equivalent positions at the boundary. The Surface Site Substitution test examines the difference in energy for the substitution of layers of Pd atoms at different depths in (111) Pt surface slabs. Errors are reported in percent difference from the value calculated with DFT.

	DFT	MD	Error [%]
$\Sigma 5$ Site Substitution			
Site 1	0.1214	-0.1982	-263.168
Site 2	-1.2127	-0.7805	-35.637
Site 3	-0.0744	-0.1982	166.257
Site 4	-1.2138	-0.7805	-35.696
(111) Surface Site Substitution			
Pt(111)-Surf	-0.4051	-0.1061	89.210
Pt(111)-SubSurf	-0.7665	0.0121	-111.389
Bulk Site Substitution			
Au in Pt(111)	2.75394	2.810275	2.046

Table 3: Coefficients for the fitting of single element potentials. The parameters are used in Eqs. 1, 2, and 3.

Coefficient	Pt	Au
E_0	-5.5056688400	-3.0330710327
r_0	2.8117394047	2.9371094370
a_m	1.5466362282	2.1869362276
λ_R	0.1625746000	0.1437112170
ρ_0	1.2851435943	1.3619497798
λ_0	0.3845403249	0.4378868737
D_e	0.3023110161	0.1162978385
r_p	5.0023688660	5.7305726517
r_d	5.0082001634	5.6306726014

Table 4: Coefficients for the fit of Eq. 2 for the binary alloy potential

Coefficient	PtAu
r_0	2.7005171343
ρ_0	0.5099937463
a_m	2.2672956035
D_e	0.3166643333
r_p	5.2909653593

Table 5: Polynomial fit to the lattice constant $a(T)$ with respect to temperature according to the form of Eq. 8.

Element	Property	A	B	C	D
Pt	$a(0 \text{ K} \leq T \leq 2000 \text{ K}) [\text{\AA}]$	9.0281×10^{-12}	-1.5472×10^{-8}	2.8564×10^{-5}	3.9757
Au	$a(0 \text{ K} \leq T \leq 1200 \text{ K}) [\text{\AA}]$	3.6985×10^{-12}	2.1535×10^{-8}	7.3391×10^{-5}	4.1537

References

- [1] Furio Ercolessi and James B. Adams. Interatomic potentials from first-principles calculations: the force-matching method. *Europhysics Letters*, 26(8):583, 1994. ISSN 0295-5075. doi: 10.1209/0295-5075/26/8/005.
- [2] Philip M. Morse. Diatomic Molecules According to the Wave Mechanics. II. Vibrational Levels. *Physical Review*, 34(1):57–64, jul 1929. ISSN 0031-899X. doi: 10.1103/PhysRev.34.57.
- [3] S. Foiles, M. Baskes, and M. Daw. Embedded-atom-method functions for the fcc metals Cu, Ag, Au, Ni, Pd, Pt, and their alloys. *Physical Review B*, 33(12):7983–7991, jun 1986. ISSN 0163-1829. doi: 10.1103/PhysRevB.33.7983.
- [4] J H Rose, J R Smith, F Guinea, and J Ferrante. Universal Features of the Equation of State of Metals. *Physical Review B*, 29(6):2963–2969, 1984. doi: 10.1103/Physrevb.29.2963.
- [5] Brian M. Adams, Keith R. Dalbey, Michael S. Eldred, David M. Gay, Laura P. Swiler, William J. Bohnhoff, John P. Eddy, and Karen Haskell. DAKOTA, a multilevel parallel object-oriented framework for design optimization, parameter estimation, uncertainty quantification, and sensitivity analysis (SAND2014-4633). 2014.
- [6] Steve Plimpton. Fast Parallel Algorithms for Short-Range Molecular Dynamics. *Journal of Computational Physics*, 117(1):1–19, 1995. doi: 10.1006/jcph.1995.1039.
- [7] Thomas Mattsson and Ann Mattsson. Calculating the vacancy formation energy in metals: Pt, Pd, and Mo. *Physical Review B*, 66(21):214110, dec 2002. ISSN 0163-1829. doi: 10.1103/PhysRevB.66.214110.
- [8] C J Smith, editor. *Smithells Metals Reference Book*. Butterworths, London, 5th edition, 1976.
- [9] N W Ashcroft and N D Mermin. *Solid State Physics*. Holt, Rinehart and Winston, New York, 1976. ISBN 9780030493461.
- [10] G Simmons and H Wang. *Single Crystal Elastic Constants and Calculated Aggregate Properties: A Handbook*. MIT Press, Cambridge, MA, 1971.
- [11] L.E. Murr. Temperature coefficient of twin-boundary energy: The determination of stacking-fault energy from the coherent twin-boundary energy in pure F.C.C. metals. *Scripta Metallurgica*, 6(3):203–208, mar 1972. ISSN 00369748. doi: 10.1016/0036-9748(72)90168-8.
- [12] R.W. Balluffi. Vacancy defect mobilities and binding energies obtained from annealing studies. *Journal of Nuclear Materials*, 69-70:240–263, feb 1978. ISSN 00223115. doi: 10.1016/0022-3115(78)90247-7.

- [13] P C J Gallagher. The Influence of Alloying, Temperature, and Related Effects on the Stacking Fault Energy. *Metallurgical Transactions*, 1(9):2429–2461, 1970. doi: 10.1007/BF03038370.
- [14] H. L. Skriver and N. M. Rosengaard. Surface energy and work function of elemental metals. *Physical Review B*, 46(11):7157–7168, sep 1992. ISSN 0163-1829. doi: 10.1103/PhysRevB.46.7157.